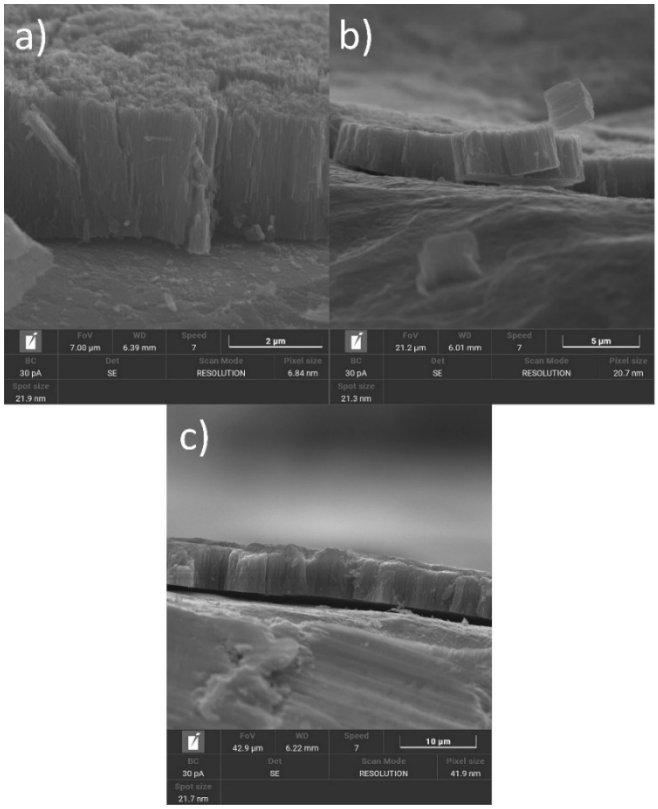


Figure S1. SEM cross-section images of a) NTO-0/40, b) NTO-0.01/60 and c) NTO-0.10/40.

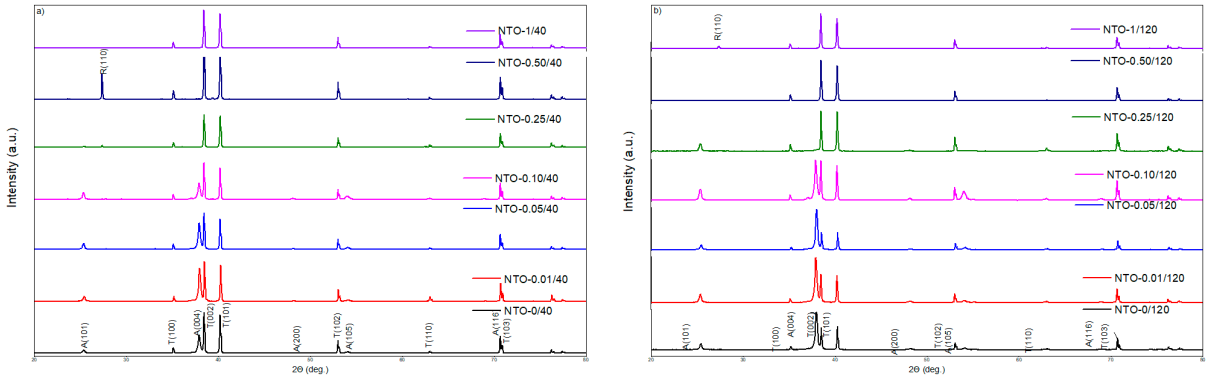


Figure S2. XRD patterns of a) NTO-x/40 and b) NTO-x/120 samples of heat-treated nanotubular titanium oxide (where x is the boric acid concentration). A – Anatase and T – Titanium.

Table S1. Unit cell parameter values of the anatase phase in the NTO, obtained by sequential annealing in air and hydrogen at 400 °C.

Lattice Parameter [Å]	Anodizing Time [min]	BA concentration in the electrolyte [M]						
		0	0.01	0.05	0.10	0.25	0.50	1
a=b	40	3.786	3.785	3.786	3.786	undetectable		
	60	3.787	3.785	3.787	3.787			
	120	3.787	3.786	3.787	3.787			
c	40	9.499	9.499	9.497	9.499	undetectable		
	60	9.503	9.499	9.498	9.503			
	120	9.501	9.500	9.502	9.503			

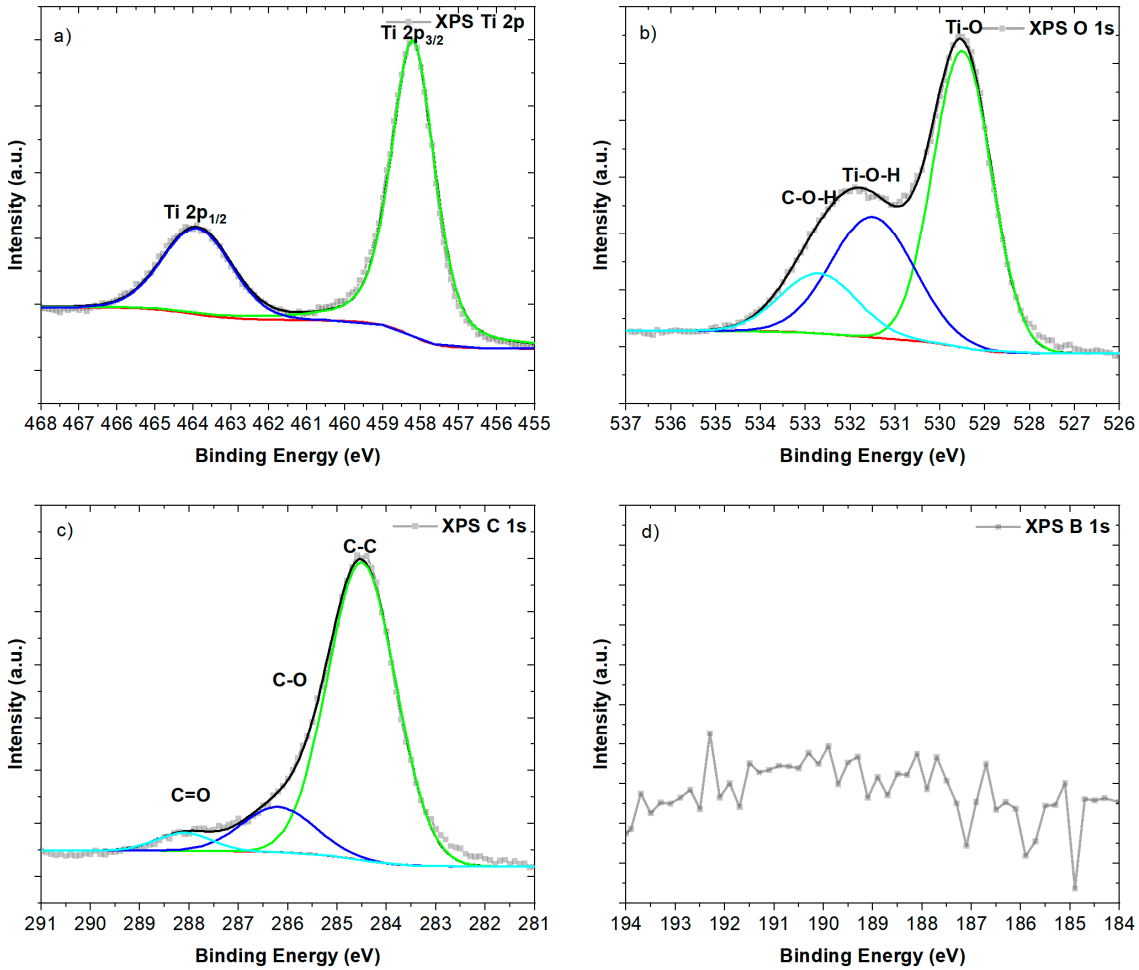


Figure S3. XPS spectra of the NTO-0/120 coating after sequential thermal treatment in air and hydrogen atmospheres: a) Ti 2p, b) O 1s, c) C 1s, and d) B 1s regions.

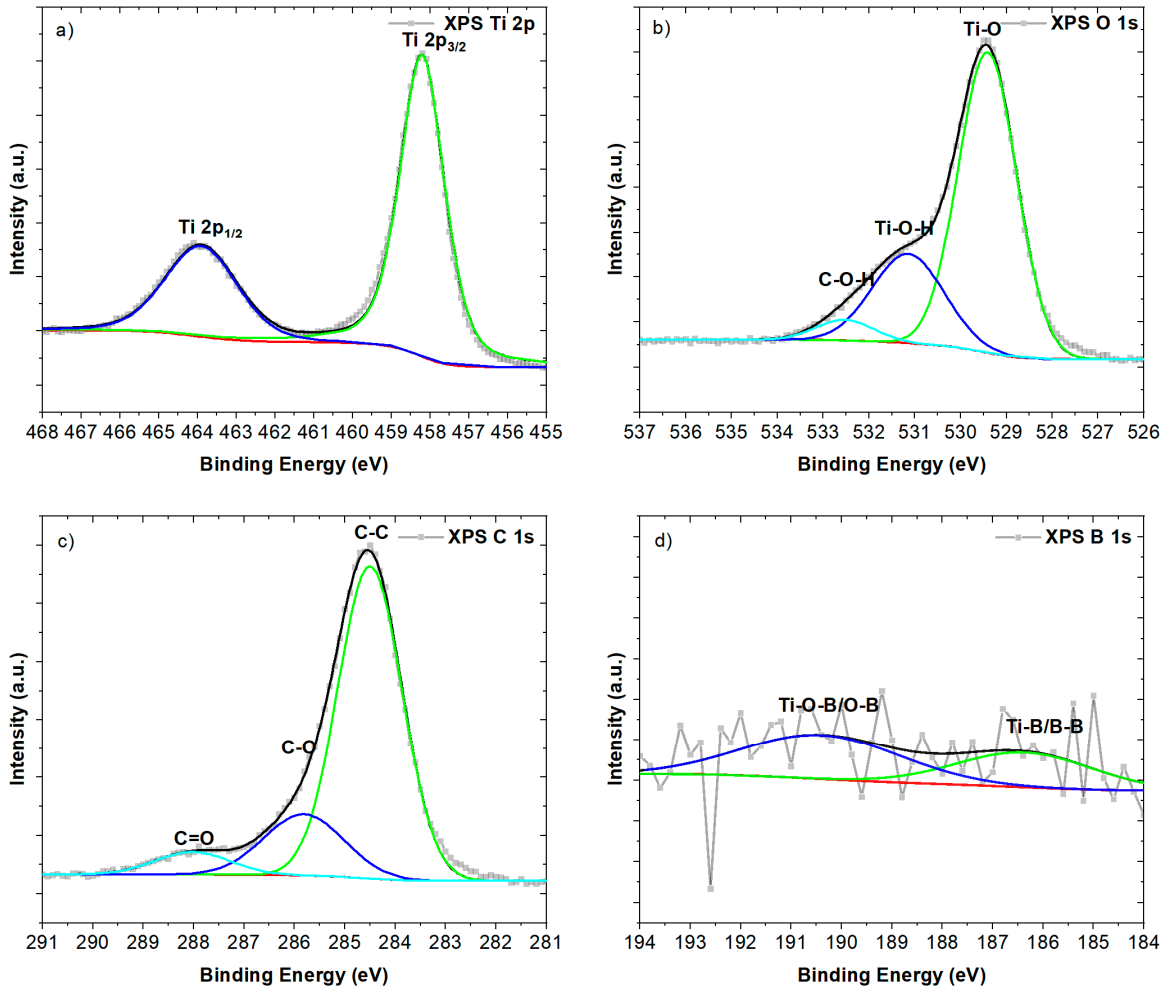


Figure S4. XPS spectra of the NTO-0.01/120 coating after sequential thermal treatment in air and hydrogen atmospheres: a) Ti 2p, b) O 1s, c) C 1s, and d) B 1s regions.

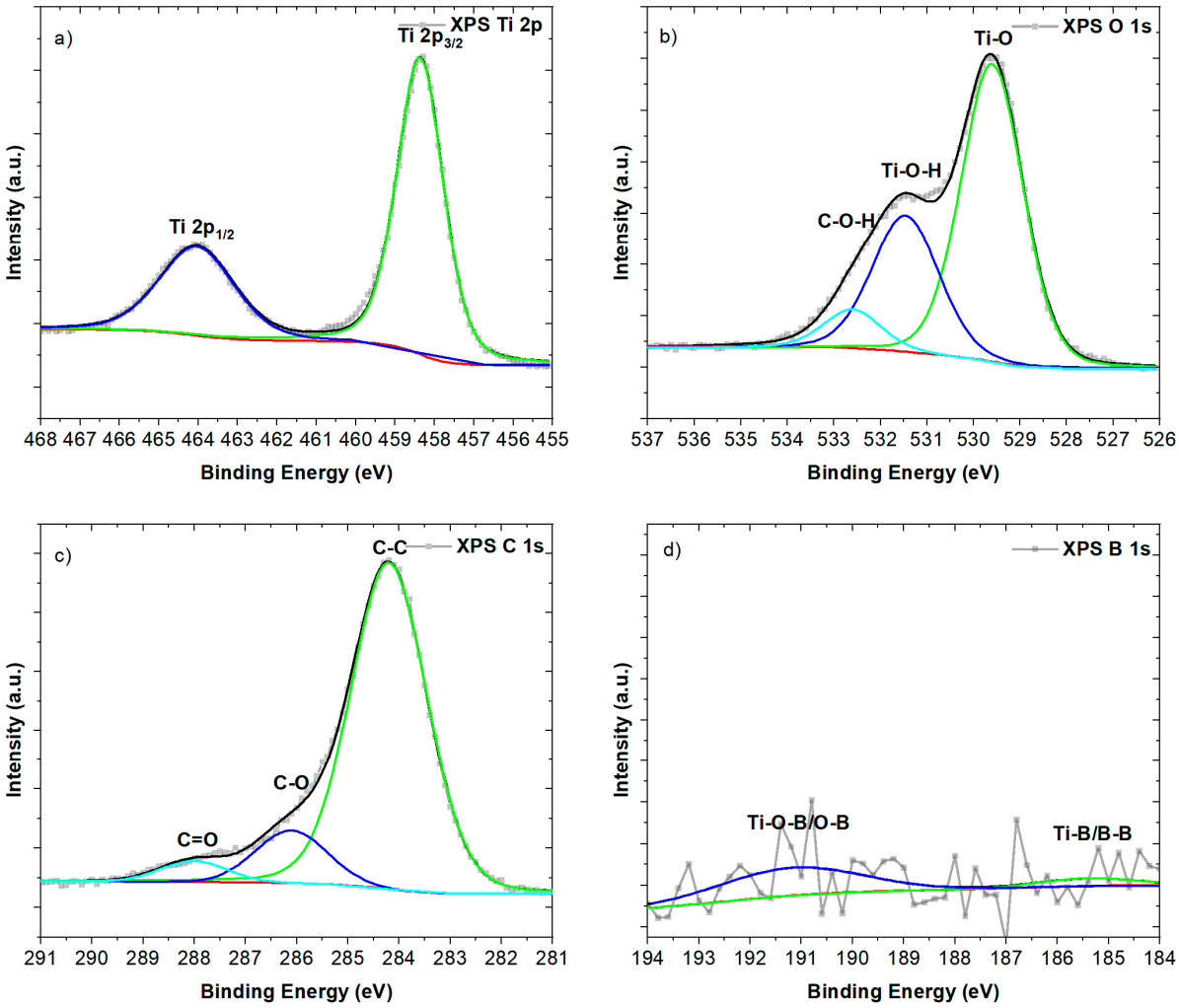


Figure S5. XPS spectra of the NTO-0.05/120 coating after sequential thermal treatment in air and hydrogen atmospheres: a) Ti 2p, b) O 1s, c) C 1s, and d) B 1s regions.

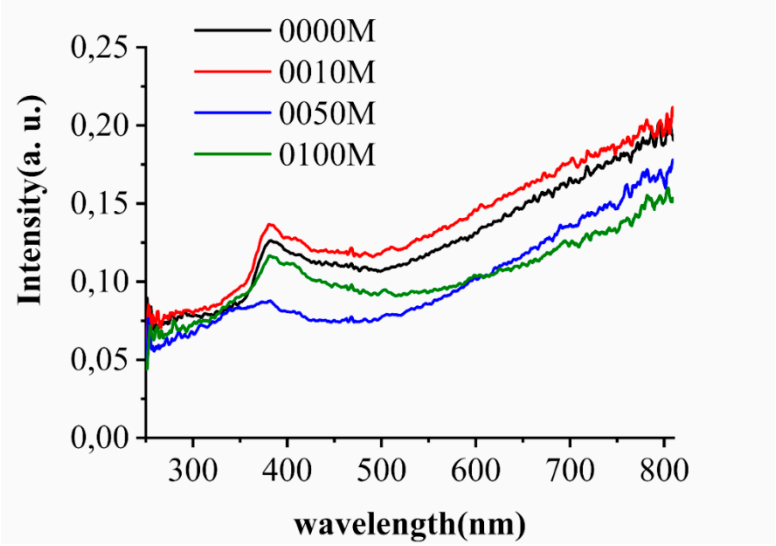


Figure S6. UV-Vis spectrum of samples NTO-0/y, NTO-0.01/y, NTO-0.05/y and NTO-0.10/y, where y = 120 min.

The complex absorption spectrum of NTO-x/y nanotubes can be represented as a linear combination of the absorption spectra $\alpha_s(h\upsilon)$ of a TiO_2 semiconductor and modifying impurities $\alpha_m(h\upsilon)$, such as Ti^{3+} oxygen vacancy and $O_2^{\bullet\bullet-}$ ion, as shown in the equation (S.1):

$$\alpha(h\upsilon) = a\cdot\alpha_s(h\upsilon) + b\cdot\alpha_m(h\upsilon) \quad \text{(S.1)}$$

where a and b contribute the corresponding components, depending on their concentration. Substituting equation (9) in (S.1) results in two equations (S.2) and (S.3):
For the direct transition:

$$(\alpha_s(h\upsilon)\cdot h\upsilon)^2 + 2\cdot\alpha_s(h\upsilon)\cdot\alpha_m(h\upsilon)\cdot(h\upsilon)^2 + (\alpha_m(h\upsilon)\cdot h\upsilon)^2 = B(h\upsilon - E_g) \quad \text{(S.2)}$$

For the indirect transition (via Taylor series expansion):

$$\left[\alpha_s(h\upsilon)^{\frac{1}{2}} + \frac{1}{2}\cdot\alpha_m(h\upsilon)\cdot\left(\frac{1}{\alpha_s(h\upsilon)}\right)^{\frac{1}{2}} - \frac{1}{8}\cdot\alpha_m(h\upsilon)^2\cdot\left(\frac{1}{\alpha_s(h\upsilon)}\right)^{\frac{3}{2}} + \frac{1}{16}\cdot\alpha_m(h\upsilon)^3\cdot\left(\frac{1}{\alpha_s(h\upsilon)}\right)^{\frac{5}{2}} + \cdots\right]\cdot$$
$$(h\upsilon)^{\frac{1}{2}} = B(h\upsilon - E_g) \quad \text{(S.3)}$$

To eliminate the impact of low energy absorption bands on the bandgap estimation, an additional condition, $\alpha_m(h\upsilon) = 0$ must be introduced. Geometrically, this is achieved by setting a baseline at the $\alpha_m(h\upsilon)$ levels in the sub-bandgap region of the Tauc plot. Consequently, equation (9) is modified and can be expressed as equations (S.4) and (S.5).

$$(\alpha_s(h\upsilon)\cdot h\upsilon)^n = B(h\upsilon - (E_g)_S) \quad \text{(S.4)}$$

or considering the use of the KM function,

$$(F(R_\infty))_S h\upsilon)^n = (E_g)_S) \quad \text{(S.5)}$$

where n=1/2 for the indirect and n=2 for the direct transition.

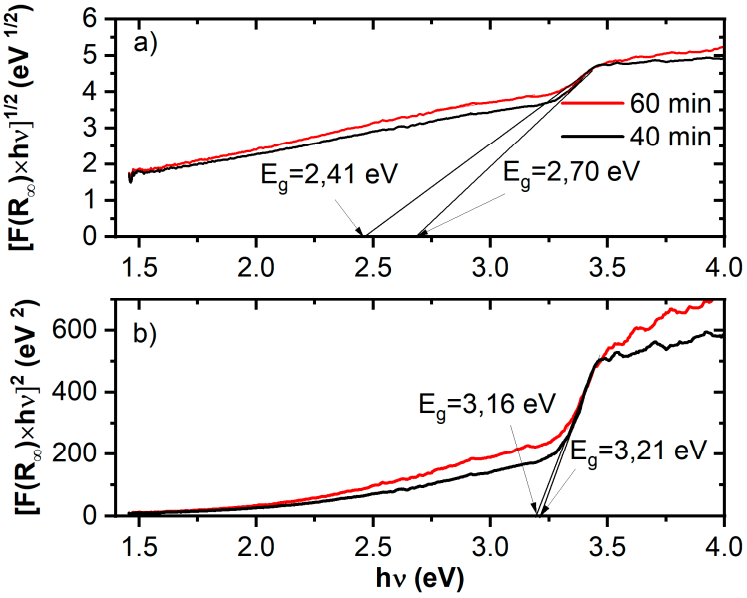


Figure S7. Example of Tauc-plot for NTO-0.05/y (A) direct and (B) indirect transitions.

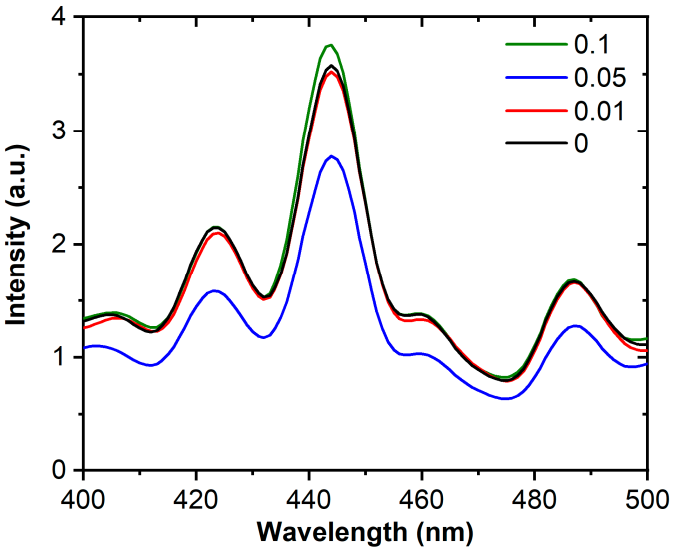


Figure S8. Example of luminescence spectra for NTO-x/120 samples (λ_{exc} = 266 nm), where x values are indicated in the plot.

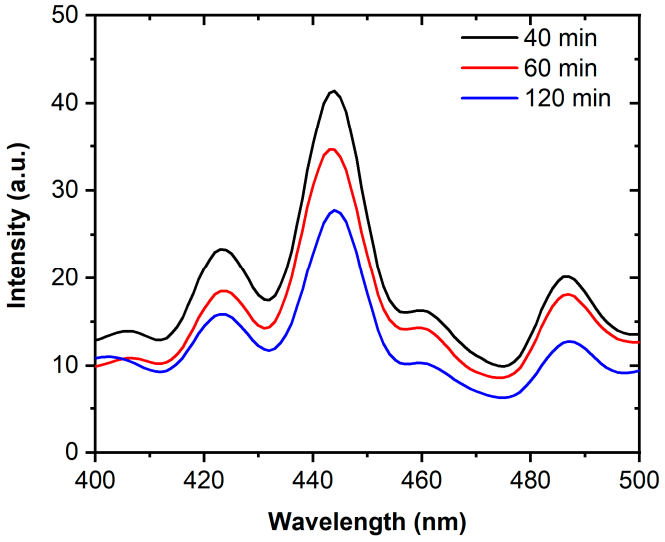


Figure S9. Example of luminescence spectra for NTO-0.05/y samples (λ_{exc} = 266 nm), where y values are indicated in the plot.

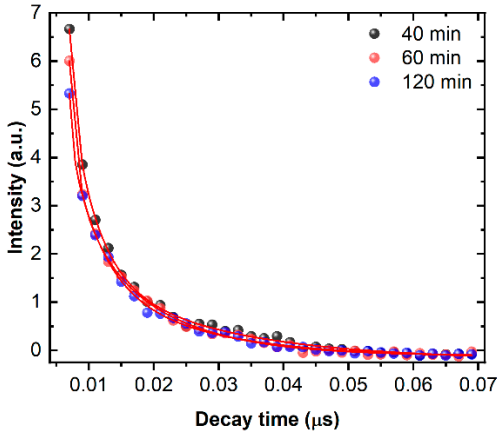


Figure S10. Example of luminescence spectra for NTO-0.05/y samples (λ_{exc} = 266 nm, λ_{em} = 441 nm), where y values are indicated in the plot.

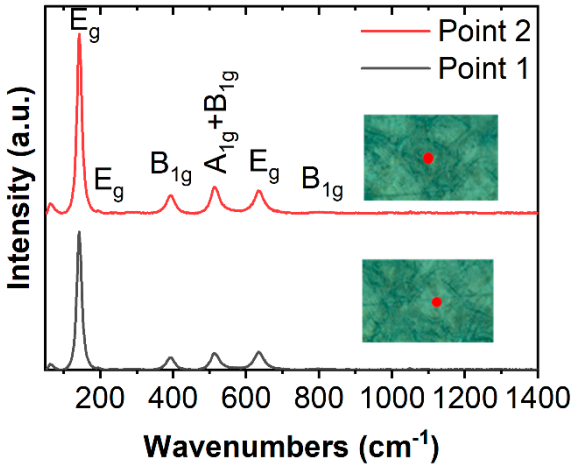


Figure S11. Example of the Raman spectra for NTO-0.05/60.

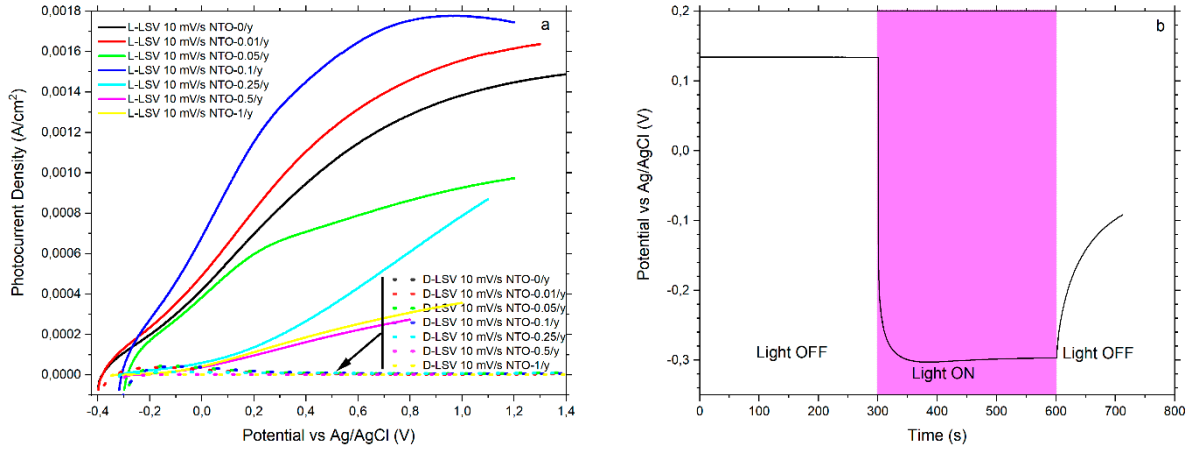


Figure S12. Example of (a) OCP–iOCP and j–V measurements obtained with a polarization sweep of 10 mV/s, and (b) "OCP–illuminated OCP" measurement for the NTO-x/120 series (where x is the boric acid concentration in the electrolyte). L-LSV refers to j–V measurements under illumination; D-LSV refers to j–V measurements in the dark. All measurements were conducted in 0.1 M KNO_3 aqueous electrolyte using a light-emitting diode with a wavelength of 365 nm.

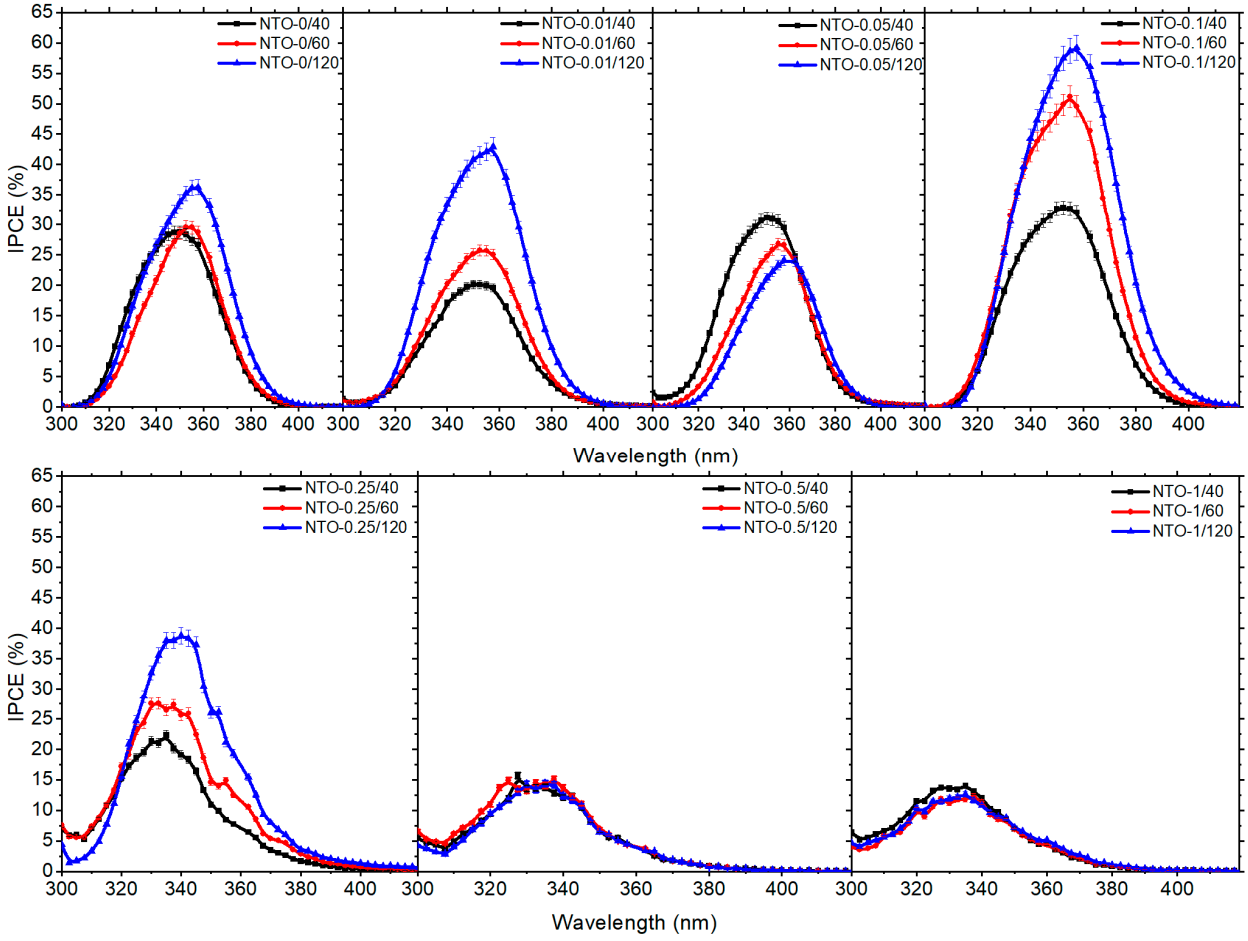


Figure S13. IPCE spectra of reduced boron-doped NTO samples.